Front. Phys. China, 2009, 4(3): 420–425
DOI 10.1007/s11467-009-0056-0

RESEARCH ARTICLE

Thermal transport associated with ballistic phonons in asymmetric quantum structures

Zong-liang LIU (刘宗良)[1,2], **Xiao-yan YU** (于晓燕)[2], **Ke-qiu CHEN** (陈克求)[2](✉)

[1] *Department of Physics, Hunan Institute of Humanities, Science and Technology, Loudi 417000, China*
[2] *Department of Applied Physics, Hunan University, Changsha 410082, China*
E-mail: keqiuchen@hnu.cn

Received February 14, 2009; accepted April 1, 2009

Using the scattering matrix method, we investigate the thermal conductance associated with ballistic phonons at low temperatures in asymmetric quantum structures. The results show that when the structure is an ideal quantum wire, the universal value $\pi^2 k_B^2/(3h)$ can be observed at very low temperatures. However, for asymmetric quantum structure, the thermal conductance is less than the universal value $\pi^2 k_B^2/(3h)$, even at $T \to 0$. The results also show that the thermal conductance is strongly dependent on the transport direction. The rectification effect can be observed in the asymmetric structure and can be adjusted by changing the structural parameters. A brief analysis of these results is given.

Keywords phonon in nanoscale structure, ballistic transport, thermal conductance

PACS numbers 63.22.-m, 73.23.Ad, 44.10.+i

1 Introduction

In recent years, progress in microfabrication and self-assembly techniques have made it possible to design various kinds of nanoscale quantum structures and devices. The thermal conductance associated with a set of discrete acoustic phonon modes in nanoscale structures, in which the wavelength of thermal phonons can be comparable to the geometrical size of the system has attracted considerable attention due to the fact that in quantum structures, thermal conductance is one of the most important parameters in controlling the performance and stability of quantum devices. The thermal conductance in various kinds of quantum structures such as superlattices [1–3], quantum wells [4, 5], one-dimensional chains [6–9], nanowires [10–17], nanotubes [18–28], graphene [29–31], and other channel shapes [32–34] were reported. Since the universal quantized thermal conductance associated with ballistic phonons at low temperatures in quantum structure was predicted theoretically [35, 36] and verified experimentally [37], the ballistic thermal transport in quantum wire structures at low temperatures is paid particular attention. For an ideal elastic wire, it is predicted theoretically that the reduced thermal conductance K/T at low temperature is quantized in an universal unit $\pi^2 k_B^2/(3h)$, analogous to the well-known $2e^2/h$ electronic conductance quantum. However, the experiment showed that the value of K/T unexpectedly decreases as the temperature increases in the range of 0.08 to 0.2 K. To understand these quantized thermal conductance phenomena, quantum wires attached with inhomogeneities such as abrupt junctions [38–40], surface roughness [41, 42], structural defects [43], and stub structures [44–49] have already been investigated. Now, it is known that the quantized thermal conductance originates from the fact that the stress-free boundary condition of ballistic phonon, allowing the propagation of the mode with $\omega = 0$ and the scattering of the structure on the long-wavelength acoustic waves in the limit $T \to 0$ is very small. The decrease of the thermal conductance at higher temperature is observed in experiment because the discontinuity can cause the additional scattering to the transport phonons and result in the decrease of the thermal conductance [34, 38–47]. When the feature size in quantum wire is smaller than the phonon mean free path in bulk material, the phonon scattering inside the structure and at the boundaries has to be considered. Therefore, the geometry details of the devices play important role in the phonon transport and thermal conductance. Recent years, the rectification effects of the heat flux have also been reported in nonlinear lattices [50, 51], in billiardlike systems [52], and in three-terminal mesoscopic dielectric systems [53] theoretically,

and it was observed in nanotube experimentally [54]. In spite of all of these advancements, a systematic understanding of the relations between structures and thermal conductance properties in quantum systems remains to be important for both foundational significance and application in devices. In particular, a systematic study for the thermal rectification effect in the asymmetric quantum structure at low temperatures is still absent.

In the present work, based on elastic model [36], we investigate thermal conductance in a asymmetric quantum structure shown in Fig. 1. Two cases are considered by changing the thermal transport direction, namely, the thermal energy transport from region I to region III, and from region III to region I. For convenience, we call the two case as case 1 and case 2, respectively. Note that the scalar model of elasticity is a rather good approximation for nanostructures at very low temperatures, and it has also been used to investigate the acoustic phonon transport and thermal conductance in various of nanoscale structures [19, 20, 28, 33, 38–40, 44–47]. The present work is aimed at searching the effects of the transport direction on the thermal conductance in asymmetric quantum structure. The results show that the thermal conductance is strongly dependent on the transport direction the rectification effect can be observed in the present structure, and it can be adjusted by changing the structural parameters.

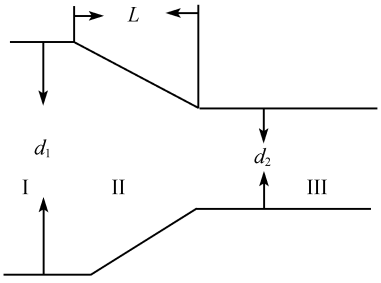

Fig. 1 Schematic illustration of a asymmetric semiconductor quantum structure. Two cases are considered by changing the thermal transport direction, namely the thermal energy transport from region I to region III, and from region III to region I. For convenience, we call the two case as case 1 and case 2, respectively.

This paper is organized as follows. In Section 2, we present a brief description of the model and the formulae used in calculations. In Section 3, we numerically investigate the properties of the thermal conductance. Finally, a summary is given in Section 4.

2 Model and formalism

We consider the model structure shown in Fig. 1, which is divided into three regions, namely, regions I, II, and III. The material in all regions is consisted of GaAs. For simplicity, we assume here that regions I, II, and III have the same thickness and are small with respect to the other dimensions and also to the wavelength of the elastic waves. It is known that thermal energy in the quantum structures is carried by a set of discrete phonon modes or vibrational modes with a finite cutoff frequency in quantum system due to transverse confinement. For the quantum structure depicted in Fig. 1, for ignore mode mixing effects that could occur at boundaries and interfaces, there exist three types of acoustic modes: longitudinal polarized P mode, vertically polarized $\boldsymbol{S}V$ mode, and horizontally polarized shear SH mode, as expounded in the elasticity textbook by Graff [55]. When P mode transports into the waveguide, the reflection at the interfaces may lead to the mode conversion, namely, its reflection wave and the transmission wave may contain both P and SV modes. The situation is similar to the SV mode. Then, the mixing of P and SV modes occurs and could lead to the appearance of the more modes [35, 56]. However, considering our assumption that regions I, II, and III have the same thickness and is small with respect to the other dimensions and also to the wavelength of the elastic waves, the horizontally polarized shear SH mode are decoupled from the phonon mode P (or SV). Li *et al.* investigated the effect of mode mixing between SV and P on the thermal conductance at low enough temperatures in a T-type structure [44]. The results show that at very low temperatures, only several lowest phonon modes can be excited, and the effect of mode mixing on the thermal conductance is very small. The thermal conductance of the SH wave has similar features to those of the P (or SV) wave. Since the present work focuses on the influences of asymmetric geometry on the acoustic phonon thermal transport at low enough temperature and also gives a comparison with the previous works [33, 39, 44–46], where only SH was considered, so in this paper, we only discuss the phonon transport and thermal conductance of SH mode. Here, we also assume that the temperatures in region I and region III are T_1 and T_3, respectively; and the temperature difference δT ($\delta T \equiv T_1 - T_3) > 0$ for case 1, and $\delta T \equiv T_3 - T_1 > 0$ for case 2) is small that we can adopt the mean temperature T ($T \equiv (T_1 + T_3)/2$) as the temperature in our calculation. For the present structure, in the ballistic transport regime, the thermal conductance at temperature T can be written in the form [35, 38]:

$$K = \frac{\hbar^2}{k_{\mathrm{B}} T^2} \sum_n \frac{1}{2\pi} \int_{\omega_n}^{\infty} \tau_n(\omega) \frac{\omega^2 \mathrm{e}^{\beta\hbar\omega}}{(\mathrm{e}^{\beta\hbar\omega} - 1)^2} \mathrm{d}\omega \qquad (1)$$

where $\tau_n(\omega)$ is the energy transmission coefficient from mode n of region I (region III) at frequency ω across all the interfaces into region III (region I) for case 1 (case 2); ω_n is the cutoff frequency of the n-th mode; $\beta = 1/(k_{\mathrm{B}}T)$, k_{B} is the Boltzman constant, T is the temperature; and $\hbar$ is the Planck's constant. A central issue in predicting the thermal conductance is then to calcu-

late the transmission coefficient $\tau_n(\omega)$. In general, elastic model [36] and lattice model [57] are applied to calculate the transmission coefficient. In the present work, we employ the elastic model to calculate the transmission coefficient of acoustic phonon. In the elastic approximation, the elastic equation of motion for SH mode is

$$\nabla^2\psi = \frac{1}{v_{SH}^2}\frac{\partial^2\psi}{\partial t^2} \tag{2}$$

where acoustic velocity v_{SH} of the SH mode is related to the mass density ρ and elastic stiffness constant C_{44}

$$v_{SH} = \sqrt{C_{44}/\rho} \tag{3}$$

To obtain the solution of Eq. (2), we first subdivide region II into a number of subregions along the transmitted direction so that each subregion is of an uniform width. Then, the solution to Eq. (2) in each region can be expressed as:

$$\Psi^{\xi}(x,y) = \sum_{n=0}^{N_\xi}(A_n^{\xi}\mathrm{e}^{\mathrm{i}k_n^{\xi}x} + B_n^{\xi}\mathrm{e}^{-\mathrm{i}k_n^{\xi}x})\phi_n^{\xi}(y) \tag{4}$$

where $\phi_n^{\xi}(y)$ represents the transverse wave function of acoustic mode in region ξ (ξ : region I, III and each subregions in II); wave vector k_n^{ξ} can be given by the energy conservation condition:

$$k_n^{\xi} = \sqrt{\frac{\omega^2}{v_\xi^2} - \frac{n^2\pi^2}{d_\xi^2}} \tag{5}$$

According to the stress-free boundary condition, the transverse wave function $\phi_n^{\xi}(y)$ in region ξ can be expressed as:

$$\phi_n^{\xi}(y) = \begin{cases} \sqrt{\dfrac{2}{d_\xi}}\cos\dfrac{n\pi}{d_\xi}(y) & (n = \text{even}) \\ \sqrt{\dfrac{2}{d_\xi}}\sin\dfrac{n\pi}{d_\xi}(y) & (n = \text{odd}) \\ \sqrt{\dfrac{1}{d_\xi}} & (n = 0) \end{cases} \tag{6}$$

where x_ξ is the reference coordinate along the x direction for region ξ, and d_ξ is the transverse dimension of region ξ. In principle, the sum over n and m includes all propagating modes and evanescent modes. In the real calculations, we take all the propagating modes and several lowest evanescent modes into account to meet the desired precision. According to boundary matching conditions, the displacement ψ and the stress $C_{44}\partial\psi/\partial x$ at the interfaces should be continuous, and the connection between the coefficients in any two adjacent subregions can be obtained by use of the scattering-matrix method [39, 58, 59]. Then, we can derive the transmission coefficient τ_n.

In the following numerical calculations, we employ the following values of elastic stiffness constant and the mass density of GaAs [60]: $c_{44}(\mathrm{GaAs}) = 5.99(10^{10}\mathrm{N}\cdot\mathrm{m}^{-2})$, and $\rho(\mathrm{GaAs}) = 5317.6\ \mathrm{kg}\cdot\mathrm{m}^{-3}$.

3 Numerical results and analyses

Figure 2(a) and (b) describe the thermal conductance divided by temperature K/T, which is reduced by the zero-temperature universal value $\pi^2k_\mathrm{B}^2/(3h)$, as a function of the temperature T for different width d_2: (a) and (b) correspond to case 1 (from wide lead to narrow lead) and case 2 (from narrow lead to wide lead), respectively. The solid, dashed, and dotted curves correspond to $d_1 = 10$, 12, and 15 nm, respectively. Here, we take $d_2 = 10$ nm and $L = 5$ nm for both cases 1 and 2. In Fig. 2(a), it can be found that when $d_1 = 10$, the structure is recovered to an ideal quantum wire, and the thermal conductance present a plateau with value $\pi^2k_\mathrm{B}^2/(3h)$ at very low temperatures. This is the universal quantized thermal conductance, as predicted theoretically [35, 36] and confirmed experimentally [37]. It is known from the previous works that the quantized thermal conductance originates from the contribution of the lowest acoustic phonon mode [39, 43]. When $d_1 > d_2$, for both case 1 and case 2, the thermal conductance plateau disappears, and the value of the thermal conductance is less than the universal value $\pi^2k_\mathrm{B}^2/(3h)$ at very low temperatures, where only the lowest mode is excited. Even at $T \to 0$, the thermal conductance is also obviously less than the universal value $\pi^2k_\mathrm{B}^2/(3h)$. This phenomenon is different from that presented in the previous reports [34, 39, 41–47], where it is suggested that in the limit $T \to 0$ the thermal conductance always approaches the universal value $\pi^2k_\mathrm{B}^2/(3h)$ and does not depend on the geometry details. Their conclusion is based on the fact that the attached scattering by the discontinuity at interfaces on the long-wavelength acoustic waves with $\omega\to 0$ is very small in the limit $T \to 0$. We think that the difference between the present structure and the previous works should result from the fact that the transversal dimension for both incident lead (region I) and output lead (region III) in the previous reports is same, while that in the present structure is not same. For the former, the attached scattering comes from the scattering region II such as stub structures [44–46, 48], structural defects [43]. In the long wavelength limit $T \to 0$, the scattering from the the discontinuity is very small, so resonant transport will occur in these structures. As a result, the reduced thermal conductance is always kept to be the universal value $\pi^2k_\mathrm{B}^2/(3h)$. However, for the latter (namely for the present structure), the scattering comes from the scattering region II, and the coupling degree between incident lead and the output lead due to

their transversal dimensions are not same. In the long wavelength limit $T \to 0$, the scattering from the output lead is always kept to be finite, so the thermal conductance is always less than the universal value $\pi^2 k_{\rm B}^2/(3h)$. Comparing Fig. 2(a) with (b), it can be found that at very low temperature, the thermal conductance in both case 1 and 2 is almost same. However, for higher temperature, where more modes than the lowest modes can be excited, the thermal conductance in case 1 is smaller than that in case 2. This can be understood. The magnitude of the thermal conductance depends on the the number of the excited modes and the scattering degree coming from the discontinuity. For case 1, the incident phonons are scatter more strongly from wide lead to narrow lead than the contrary direction (case 2), but at same temperature, the number of the excited phonon modes is larger than that of case 2 because the transversal dimension in incident region is larger than that of the case. The combined effects may lead to the thermal conductance in case 1 being smaller than that in case 2.

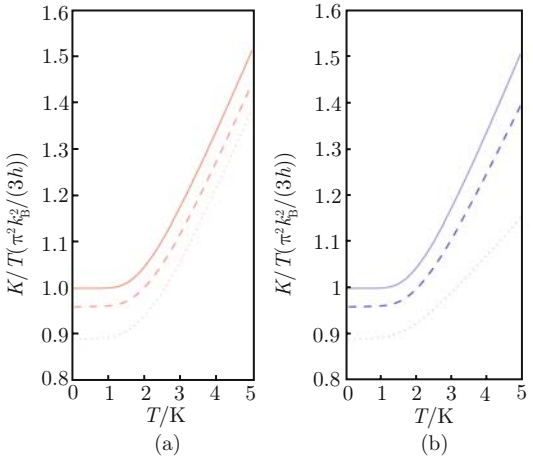

Fig. 2 The thermal conductance divided by temperature K/T, which is reduced by the zero-temperature universal value $\pi^2 k_{\rm B}^2/(3h)$, as a function of the temperature T for different width d_2: **(a)** and **(b)** correspond to case 1 and case 2, respectively. The solid, dashed and dotted curves correspond to $d_1 = 10$, 12, and 15 nm, respectively. Here, we take $d_2 = 10$ nm and $L = 5$ nm.

In Fig. 3(a) and (b), we give the thermal conductance dependence on length L for different temperature. (a) and (b) correspond to case 1 and case 2, respectively. The solid, dashed, dotted, and dash-dotted curves correspond to $T = 1$, 2, 3, and 4 (k), respectively. Here, we take $d_1 = 20$ nm and $d_2 = 10$ nm for both case 1 and 2. In Fig. 3(a) and (b), it is seen clearly that the thermal conductance is increased with the increase of the length L. This can be easily understood. When the length L becomes longer, the incline degree of the scattering region II becomes more smaller scattering to phonon is also reduced, and so, the thermal is increased. Comparing Fig. 3(a) with (b), it can be found that for same length L, the thermal conductance from wide lead to narrow lead (case 1) is obviously smaller than that from the opposite direction (case 2), and the for higher temperature, the difference is bigger. This means that the rectification effect is obvious, especially for the higher temperature and smaller L. This appears to be important for applications in thermal rectification devices. These results also indicate that the thermal conductance can be adjusted by changing the length L.

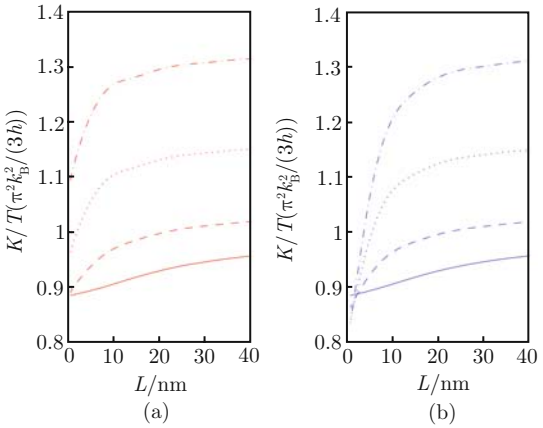

Fig. 3 The thermal conductance dependence on length L for different temperature. **(a)** and **(b)** correspond to case 1 and case 2, respectively. The solid, dashed, dotted, and dash-dotted curves correspond to $T = 1$, 2, 3, and 4 (k), respectively. Here, we take $d_1 = 20$ nm and $d_2 = 10$ nm.

Figure 4(a) and (b) describe the thermal conductance dependence on the transversal dimension d_1 for different temperature T. (a) and (b) correspond to case 1 and case 2, respectively. The solid, dashed, dotted curves correspond to $T = 1$, 2, and 3 (k), respectively. Here, we take $d_2 = 10$ nm and $L = 5$ nm for both cases 1 and 2. When $d_1 = d_2$, the structure is recovered to an ideal quantum wire, so the thermal conductance is same for both case 1 and case 2. At $T = 1$ k, only the lowest mode can be excited in the structure, the universal ther-

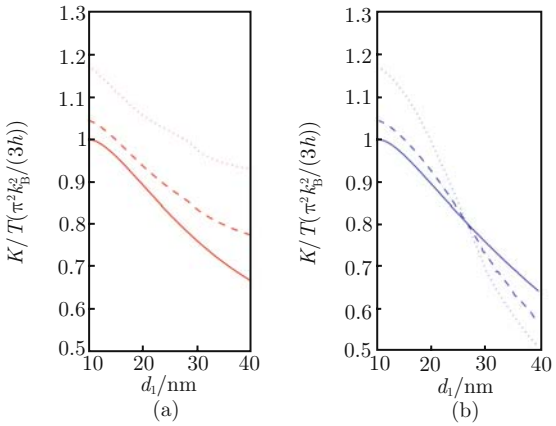

Fig. 4 The thermal conductance dependence on the transversal dimension d_1 for different temperature T. **(a)** and **(b)** correspond to case 1 and case 2, respectively. The solid, dashed, dotted curves correspond to $T = 1$, 2,and 3 (k), respectively. Here, we take $d_2 = 10$ nm and $L = 5$ nm.

mal conductance $\pi^2 k_B^2/(3h)$ can be observed. In Figs. 4(a) and (b), it can be found that the thermal conductance is decreased with the increase of d_1 in both case 1 and case 2, but the change of the thermal conductance is more faster in case 2 than in case 1, which show the the rectification effect is possible in the structure. Especially, for the higher temperature and bigger d_1, the rectification effect is more obvious. In Fig. 4(a), we can see that the thermal conductance is increased monotonically with the increase of the temperature, while in Fig. 4(b), we find that the reverse case occurs for bigger d_1. This show that when $d_1 \neq d_2$, the thermal conductance is strongly dependent on the transport direction.

4 Summary

In the present work, we have presented a numerical study of the thermal conductance associated with ballistic phonon in asymmetric semiconductor quantum structures by using a scalar model of elasticity. The results show that when $d_1 = d_2$, namely, the structure is an ideal quantum wire, and the universal value $\pi^2 k_B^2/(3h)$ and quantum plateau can be observed at very low temperatures, where only the lowest mode is excited. When $d_1 \neq d_2$, the thermal conductance plateau disappears, and the value of the thermal conductance is less than the universal value $\pi^2 k_B^2/(3h)$ at very low temperatures. Even at $T \to 0$, the thermal conductance is also obviously less than the universal value $\pi^2 k_B^2/(3h)$. The results also show that when $d_1 \neq d_2$, the thermal conductance is strongly dependent on the transport direction, the rectification effect is obvious in the structure, and it can be adjusted by changing the structural parameters. It is suggested that the present structure may be useful for applications in thermal rectification devices.

Acknowledgements This work was supported by the National Natural Science Foundation of China (Grant Nos. 10674044 and 10774042), the Specialized Research Fund for the Doctoral Program of Higher Education of China (Grant No. 200805320011), and the Science Research Fund of Educational Bureau of Hunan Province of China (Grant No. 08C463).

References

1. G. Chen, Phys. Rev. B, 1998, 57: 14958
2. W. E. Bies, R. J. Radtke, and H. Ehrenreich, J. Appl. Phys., 2000, 88: 1498
3. M. V. Simkin and G. D. Mahan, Phys. Rev. Lett., 2000, 84: 927
4. D. Song and G. Chen, Appl. Phys. Lett., 2004, 84: 687
5. D. Z. A. Chen, A. Narayanaswamy, and G. Chen, Phys. Rev. B, 2005, 72: 155435
6. B. W. Li, L. Wang, and B. B. Hu, Phys. Rev. Lett., 2002, 88: 223901
7. B. W. Li, G. Casati, J. Wang, and T. Prosen, Phys. Rev. Lett., 2004, 92: 254301
8. J. S. Wang, Phys. Rev. Lett., 2007, 99: 160601
9. J. S. Wang, N. Zen, J. Wang, and C. K. Gan, Phys. Rev. B, 2007, 75: 061128
10. B. A. Glavin, Phys. Rev. Lett., 2001, 86: 4318
11. J. Zou and A. Balandin, J. Appl. Phys., 2001, 89: 2932
12. W. Fon, K. C. Schwab, J. M. Worlock, and M. L. Roukes, Phys. Rev. B, 2002, 66: 045302
13. D. Y. Li, Y. Y. Wu, P. Kim, L. Shi, P. D. Yang, and A. Majumdar, Appl. Phys. Lett., 2003, 83: 2934
14. R. G. Yang, G. Chen, and M. S. Dresselhaus, Phys. Rev. B, 2005, 72: 125418
15. O. Chiatti, J. T. Nicholls, Y. Y. Proskuryakov, N. Lumpkin, I. Farrer, and D. A. Ritchie, Phys. Rev. Lett., 2006, 97: 056601
16. J. Wang and J. S. Wang, Appl. Phys. Lett., 2007, 90: 241908
17. C. Guthy, C. Y. Nam, and J. E. Fischer, J. Appl. Phys., 2008, 103: 064319
18. P. Kim, L. Shi, A. Majumdar, and P. L. McEuen, Phys. Rev. Lett., 2001, 87: 215502
19. N. Mingo and D. A. Broido, Phys. Rev. Lett., 2005, 95: 096105
20. N. Mingo and D. A. Broido, Nano Lett., 2005, 5: 1221
21. H. Y. Chiu, V. V. Deshpande, H. W. Ch. Postma, C. N. Lau, C. Miko, L. Forro, and M. Bockrath, Phys. Rev. Lett., 2005, 95: 226101
22. J. S. Wang, J. Wang, and N. Zeng, Phys. Rev. B, 2006, 74: 033408
23. J. S. Wang, N. Zeng, J. Wang, and C. K. Gan, Phys. Rev. E, 2007, 75: 061128
24. T. Yamamoto, Y. Nakazawa, and K. Watanabe, New J. Phys., 2007, 9: 245
25. G. Wu and B. W. Li, Phys. Rev. B, 2007, 76: 85424
26. W. Zhang, N. Mingo, and T. S. Fisher, Phys. Rev. B, 2007, 76: 195429
27. Z. L. Wang, D. W. Tang, X. B. Li, X. H. Zheng, W. G. Zhang, L. X. Zheng, Y. T. Zhu, A. Z. Jin, H. F. Yang, and C. Z. Gu, Appl. Phys. Lett., 2007, 91: 123119
28. N. Mingo D. A. Stewart, D. A. Broido, and D. Srivastava, Phys. Rev. B, 2008, 77: 033418
29. K. Satio, J. Nakamura, and A. Natori, Phys. Rev. B, 2007, 76: 115409
30. M. Morooka, T. Yamamoto, and K. Watanabe, Phys. Rev. B, 2008, 77: 033412
31. J. Zimmermann, P. Pavone, and G. Cuniberti, Phys. Rev. B, 2008, 78: 045410
32. Q. F. Sun, P. Yang, and H. Guo, Phys. Rev. Lett., 2002, 89: 175901
33. W. X. Li, K. Q. Chen, W. H. Duan, J. Wu, and B. L. Gu, Appl. Phys. Lett., 2004, 85: 822
34. F. Xie, K. Q. Chen, Y. G. Wang, Q. Wan, B. S. Zou, and Y. Zhang, J. Appl. Phys., 2008, 104: 054312
35. L. G. C. Rego and G. Kirczenow, Phys. Rev. Lett., 1998, 81: 232
36. M. P. Blencowe, Phys. Rev. B, 1999, 59: 4992
37. K. Schwab, E. A. Henriksen, J. M. Worlock, and M. L. Roukes, Nature (London), 2000, 404: 974
38. M. C. Cross and R. Lifshitz, Phys. Rev. B, 2001, 64: 85324

39. W. X. Li, K. Q. Chen, W. H. Duan, J. Wu, and B. L. Gu, J. Phys. D: Appl. Phys., 2003, 36: 3027
40. C. M. Chang and M. R. Geller, Phys. Rev. B, 2005, 71: 125304
41. D. H. Santamore and M. C. Cross, Phys. Rev. Lett., 2001, 87: 115502
42. D. H. Santamore and M. C. Cross, Phys. Rev. B, 2001, 63: 184306
43. K. Q. Chen, W. X. Li, W. H. Duan, Z. Shuai, and B. L. Gu, Phys. Rev. B, 2005, 72: 045422
44. W. X. Li, K. Q. Chen, W. H. Duan, J. Wu, and B. L. Gu, J. Phys.: Condens. Matter, 2004, 16: 5049
45. W. Q. Huang, K. Q. Chen, Z. Shuai, L. L. Wang, W. Y. Hu, and B. S. Zou, J. Appl. Phys., 2005, 98: 093524
46. L. M. Tang, L. L. Wang, K. Q. Chen, W. Q. Huang, and B. S. Zou, Appl. Phys. Lett., 2006, 88: 163505
47. P. Yang, Q. F. Sun, H. Guo, and B. B. Hu, Phys. Rev. B, 2007, 75: 235319
48. X. F. Peng, K. Q. Chen, B. S. Zou, and Y. Zhang, Appl. Phys. Lett., 2007, 90: 193502
49. F. Xie, K. Q. Chen, Y. G. Wang, and Y. Zhang, J. Appl. Phys., 2008, 103: 084501
50. B. W. Li, L. Wang, and G. Casati, Phys. Rev. Lett., 2004, 93: 184301
51. B. B. Hu, L. Yang, and Y. Zhang, Phys. Rev. Lett., 2006, 97: 124302
52. J. P. Eckmann and C. Mejia-Monasterio, Phys. Rev. Lett., 2006, 97: 094301
53. Y. Ming, Z. X. Wang, Q. Li, and Z. J. Ding, Appl. Phys. Lett., 2007, 91: 143508
54. C. W. Chang, D. Okawa, A. Majumdar, and A. Zettl, Science, 2006, 314: 1121
55. K. Graff, Wave Motion in Elastic Solids, New York: Dover, 1991
56. Y. Tanaka, F. Yoshida, and S. Tamura, Phys. Rev. B, 2005, 71: 205308
57. J. S. Wang, J. Wang, and J. T. Lu, Eur. Phys. J. B, 2008, 62: 381
58. H. Q. Xu, Phys. Rev. B, 1995, 52: 5803
59. H. Q. Xu, Appl. Phys. Lett., 2002, 80: 853
60. O. Madelung, Semiconductors: Group IV Elements and III-V Compounds, Berlin: Springer, 1982